

Multi-Label Contrastive Learning : A Comprehensive Study

Alexandre Audibert^{1,*}, Aurélien Gauffre^{1,*}, and Massih-Reza Amini¹

¹Université Grenoble Alpes

^{*}Equal contribution

December 3, 2024

Abstract

Multi-label classification, which involves assigning multiple labels to a single input, has emerged as a key area in both research and industry due to its wide-ranging applications. Designing effective loss functions is crucial for optimizing deep neural networks for this task, as they significantly influence model performance and efficiency. Traditional loss functions, which often maximize likelihood under the assumption of label independence, may struggle to capture complex label relationships. Recent research has turned to supervised contrastive learning, a method that aims to create a structured representation space by bringing similar instances closer together and pushing dissimilar ones apart. Although contrastive learning offers a promising approach, applying it to multi-label classification presents unique challenges, particularly in managing label interactions and data structure.

In this paper, we conduct an in-depth study of contrastive learning loss for multi-label classification across diverse settings. These include datasets with both small and large numbers of labels, datasets with varying amounts of training data, and applications in both computer vision and natural language processing.

Our empirical results indicate that the promising outcomes of contrastive learning are attributable not only to the consideration of label interactions but also to the robust optimization scheme of the contrastive loss. Furthermore, while the supervised contrastive loss function faces challenges with datasets containing a small number of labels and ranking-based metrics, it demonstrates excellent performance, particularly in terms of Macro-F1, on datasets with a large number of labels.

Finally, through gradient analysis of standard contrastive loss in multi-label classification, along with insights from previous work, we develop a new competitive loss function that removes certain gradient components to prevent undesirable behavior and improve performance.

1 Introduction

The field of multi-label classification (MLC) has emerged as a fundamental paradigm in machine learning, receiving considerable attention in both computer vision (CV) and natural language processing (NLP). Unlike traditional single-label classification, MLC tackles the more complex task of associating multiple labels to individual instances, thereby better capturing the intricacies of real-world scenarios. In computer vision applications, MLC has proven successful in advancing various domains, from scene understanding and object detection to medical image analysis

[1]. The ability to simultaneously identify multiple attributes or objects within a single image has significantly enhanced the capabilities of automated visual recognition systems. Similarly, NLP applications have made MLC indispensable for tasks requiring nuanced understanding of text. Applications include sentiment analysis, news categorization, legal or medical document classification. [2, 3].

Despite sharing similarity to multi-class classification, multi-label classification comes with several unique challenges. One key issue is label imbalance: MLC labels often exhibit a long-tailed distribution, where a few labels appear frequently, while the majority of labels appear only a limited number of times. This challenge is amplified by the imbalance between positive and negative labels, as instances tend to have significantly more negative than positive labels on average. Another challenge is the varying number of labels per instance, which can vary from case to case. Furthermore, the label space is often sparse, with specific labels that may never occur together, which must be taken into account when developing the method. Finally, label correlations present an additional challenge, as these interdependencies must be carefully considered in MLC approaches.

Over the years, various strategies have been developed to address these challenges, with a particular focus on understanding and modeling interactions between labels. One common approach involves graph-based methods that capture label dependencies within structured representations [4, 5, 6]. Another method transforms the classification task into a generative process, where the prediction of one label informs the likelihood of subsequent labels [7, 8]. Regularization loss functions are also employed to directly account for label dependencies, ensuring better representation of inter-label relationships [9, 10].

Label interactions can also be managed by incorporating external knowledge, such as hierarchical structures, which provide supplementary information that enhances model performance [11, 12]. Additionally, recent research has focused on developing label representations that integrate attention mechanisms, allowing models to pinpoint specific areas of a document or image relevant to each label [1, 13, 14].

In the early stages of deep learning, the primary objective was to maximize log-likelihood, which led to the widespread use of the Binary Cross-Entropy (BCE) loss function for multi-label classification tasks. This approach relies on binary relevance, where each label is predicted independently.

Since BCE is elementary, numerous studies have introduced enhancements to improve its performance. However, these modifications often alter the strictly probabilistic nature of BCE, either by adjusting its gradient dynamics [15, 16] or by prioritizing the ranking perspective of classification tasks [17].

To address these intricate dependencies more effectively, this paper introduces a new contrastive learning loss as an alternative to conventional methods. Contrastive approaches are particularly motivated by their ability to account for label co-occurrence through instance interactions, an inductive bias that can significantly enhance prediction accuracy.

Unlike previous methods that primarily optimize logits, contrastive approaches operate directly on feature representations, aiming to shape the representation space itself. This process involves two stages: the first stage trains the model using contrastive learning to capture effective features, while the second stage involves training a linear classifier with the backbone frozen on the learned features (linear evaluation) or fine-tuning the whole model.

Until recently, applying contrastive methods to multi-label tasks offered challenges, including managing long-tailed distributions and defining suitable positive pairs [18]. Recent works have introduced new strategies—such as varying degrees of attraction between positive pairs and adjusting for label frequency within the batch—to address these complexities [18, 19]. Furthermore, incorporating label prototypes has enabled contrastive loss to outperform traditional binary cross-entropy [20].

Despite these advances, fully understanding the mechanism of contrastive learning within the multi-label context remains challenging. The introduction of prototypes adds complexity, raising questions about whether instance interactions alone drive performance gains or if the combination of prototypes with contrastive learning is essential. Moreover, combining contrastive learning with cross-entropy in multi-class settings has proven highly efficient even with limited data [21], suggesting that further study of contrastive learning in multi-label classification with reduced data could yield valuable insights.

The contributions of this work are the following:

1. **Comprehensive analysis of contrastive losses:** We present an in-depth study of various contrastive loss functions for multi-label classification across diverse settings. This includes examining model performance when training from scratch, handling datasets with limited label availability, training on subsets of data, and utilizing full datasets.
2. **Insights into contrastive learning performance:** We provide empirical evidence showing that the efficacy of contrastive learning in MLC is due not only to modeling label interactions but also to robust optimization properties inherent in contrastive approaches.
3. **Investigation of limitations:** Our findings indicate that contrastive learning approaches demonstrate a more significant performance advantage in datasets with a higher number of labels and more complex label interactions. This suggests that the relative effectiveness of contrastive and non-contrastive methods is closely tied to the dataset label interaction.
4. **A novel contrastive loss function:** Building on insights from our analysis, we propose a new contrastive loss function that incorporates lessons learned from previous research. We introduce a novel regularization technique based on gradient analysis, which enhances efficiency and establishes state-of-the-art performance in multi-label classification tasks.

2 Related Work

In this section, we review related work on classical supervised loss functions and examine prior studies on contrastive learning within the domains of computer vision and natural language processing for multi-label classification.

2.1 Supervised Loss Functions for Multi-Label Classification

For many years, the binary cross-entropy loss function has been the most commonly used approach for multi-label classification. Based on log-likelihood maximization, BCE offers the advantage of providing a probability score associated to each label. Numerous studies have been conducted to enhance this loss function, often focusing on optimizing gradient properties. One such improvement is the *focal loss* [15], which enhances BCE by emphasizing instances that are most challenging to predict. It achieves this by introducing a modulating factor that depends on a hyperparameter γ , which allows the model to down-weight the loss for well-classified instances, thereby focusing more on hard-to-classify examples. As a result, focal loss is particularly effective for rare labels within long-tailed distributions, which are often more challenging to classify.

However, in multi-label classification, most of the labels are absent in any given particular example, resulting in gradients dominated by negative labels. To address this, the *asymmetric loss* [16] builds upon focal loss by introducing two key modifications. Like focal loss, asymmetric loss includes a down-weighting component which is applied however with two distinct factors, γ_+ and γ_- , to weight positive and negative labels asymmetrically. This setup allows

the model to focus more on challenging positive labels while reducing the influence of negative labels. Additionally, to further account for the high contribution of negative sample to the loss, asymmetric loss introduces a hard threshold mechanism, which removes the gradient contribution from very easy negative samples.

Other loss functions aim to improve the ranking of labels for each instance. One of the most notable one among these, is the *Log-Sum-Exp Pairwise* (LSEP) function [22], which is specifically designed to ensure that logits for relevant labels associated with an instance are higher than those for irrelevant labels. It incorporates a pairwise comparison between positive and negative logits, applying a penalty whenever a negative logit approaches or exceeds a positive one, thereby encouraging a clear score separation that improves label ranking.

The primary limitation of the LSEP loss is that it cannot directly predict whether a label is present or absent. To address this, the *Zero-bounded Log-sum-exp and Pairwise Rank-based* (ZLPR) loss function [17] was proposed. ZLPR has proven highly successful by extending LSEP with a fixed threshold: positive logits must exceed this threshold, while negative logits must remain below it, enabling a direct estimation of the probability of a label’s presence or absence.

2.2 Supervised Contrastive Learning

Contrastive learning has emerged as a powerful representation learning technique, initially designed to learn unsupervised representation of examples by grouping similar ones and separating dissimilar ones [23, 21]. By optimizing instance-level similarities and differences in representation space, contrastive methods encourage models to capture meaningful patterns in data, even without label supervision. Supervised contrastive learning, pioneered by *SupCon* [24], builds upon classical contrastive loss by adapting it from a self-supervised to a supervised paradigm, by simply incorporating label information. Traditional self-supervised contrastive learning constructs the representation space by bringing the embeddings of anchor points closer to those of positive samples (typically an augmented view of the same instance) while pushing them away from the embeddings of negative samples. In supervised contrastive learning, however, positive samples are defined as instances that share the same class as the anchor, using label information to enhance intra-class similarity.

Studies have compared the *SupCon* loss to the widely used cross-entropy loss. In balanced conditions and under mild encoder assumptions, both loss functions converge to similar representations [25]. However, supervised contrastive loss demonstrates superior generalization due to its ability to create more discriminative representations by clustering same-class samples more effectively than cross-entropy [25]. This behavior is particularly advantageous in complex feature spaces, where enhancing intra-class compactness results in better class separation. Originally emerging from the field of computer vision [24, 25], supervised contrastive learning has also demonstrated remarkable performance in NLP tasks [26, 27].

Despite its success in balanced settings, its application to unbalanced scenarios remains challenging. Real-world data often exhibit long-tailed distributions, which distort the representation space and amplify the dominance of majority classes. To counter this, re-weighting techniques and class prototypes have been proposed to balance the representation space by reducing the loss emphasis on majority classes or introducing stable class-specific anchors, respectively [28, 29]. These approaches aim to ensure that the learned representations remain robust and generalizable, even under distributional imbalances.

2.3 Supervised Contrastive Learning for Multi-label Classification

Several studies combine contrastive learning with classical loss functions. For example, in natural language processing, [10, 30] introduced supervised contrastive losses paired with binary

cross-entropy to enhance semantic representations of instances.

For both CV and NLP, [31] adopt a variational auto-encoder framework to align probabilistic embedding spaces for labels and features. Although highly effective, this method employs multiple loss functions alongside the contrastive loss, making it difficult to isolate its individual contribution.

Other approaches incorporate external knowledge about labels, such as hierarchical structures, to design supervised contrastive losses [32, 33, 34]. By leveraging hierarchical information, these methods simplify the definition of similarity between instances, improving both efficiency and clarity in the contrastive loss design.

Finally, some studies [35, 34] employ attention mechanisms to derive distinct representations for each label and apply contrastive loss within the batch to representations of the same label. These techniques emphasize learning label-specific features for contrastive optimization.

Our work distinguishes itself by focusing on the exploration of simple contrastive loss functions that utilize a single representation for all labels, without relying on hierarchical assumptions or combining them with standard loss functions.

3 Multi-Label Contrastive learning

In this section, we start by outlining the motivation and key challenges associated with multi-label classification. Following this, we introduce the necessary notations and present the state of the art in multi-label classification, along with key insights from previous work.

3.1 Motivation and Challenge

The application of contrastive learning to multi-label classification offers an intriguing research direction. Contrastive learning has the advantage of operating directly on hidden representations and can capture label interactions through relationships among instances. However, extending traditional supervised contrastive learning [24] to multi-label classification presents significant challenges. The primary difficulty lies in appropriately defining positive pairs, which becomes increasingly complex due to the detailed information required within the multi-label framework. Additionally, labels often follow a long-tailed distribution, where a few labels are associated with many instances, while many labels are linked to only a few instances. This imbalance is challenging in the multi-class setting but is even more pronounced in the multi-label context. In multi-label scenarios, long-tail labels are often associated with head labels, and signals from these head labels can overshadow those from the tail labels.

3.2 General Notations

In the following, let B denote the set of indices for the examples in a batch, \mathcal{B} denotes the set of hidden representations $\mathcal{B} = \{\mathbf{z}_i\}_{i=1}^{|B|}$, and L represents the number of labels. The hidden representation of the i^{th} instance in a batch is denoted by \mathbf{z}_i . The associated label vector for example i is $\mathbf{y}_i \in \{0, 1\}^L$, where y_i^j refers to its j^{th} element. $\Delta(\mathbf{z}_i) = \{k \in [1, L] \mid y_i^k = 1\}$ represents the set of labels for example i ; $P(j, i) = \{\mathbf{z}_l \in \mathcal{B} \mid y_l^j = 1\} \setminus \mathbf{z}_i$ represents the set of representations for examples having label j , excluding the representation of example i . We also define a set of L trainable label prototypes, $C = \{\mathbf{c}_i \mid i \in \{1, \dots, L\}\}$. For the sake of presentation, we use the dot product instead of tempered cosine similarity to represent contrastive losses and perform derivative calculations. However, it is important to keep in mind that, in practice, $\mathbf{z}_i \cdot \mathbf{z}_j = \frac{\langle \mathbf{z}_i, \mathbf{z}_j \rangle}{\tau \|\mathbf{z}_i\| \|\mathbf{z}_j\|}$, where τ denotes the temperature.

3.3 State-of-the-art Multi-Label Contrastive Loss Functions

One of the primary losses proposed for MLC, denoted as \mathcal{L}_{Base} , is a simple extension of the *SupCon* loss [24]. It incorporates an additional term to model the interaction between labels based on the Jaccard Similarity [18].

$$\mathcal{L}_{Base} = -\frac{1}{|B|} \sum_{\mathbf{z}_i \in \mathcal{B}} \frac{1}{N(i)} \sum_{\mathbf{y}_j \in \mathcal{B} \setminus \mathbf{z}_i} \frac{|\mathbf{y}_i \cap \mathbf{y}_j|}{|\mathbf{y}_i \cup \mathbf{y}_j|} \log \left(\frac{\exp(\mathbf{z}_i \cdot \mathbf{z}_j / \tau)}{\sum_{\mathbf{z}_k \in \mathcal{B} \setminus \mathbf{z}_i} \exp(\mathbf{z}_i \cdot \mathbf{z}_k / \tau)} \right), \quad (1)$$

where $N(i)$ is the normalization term defined as:

$$N(i) = \sum_{j \in \mathcal{B} \setminus i} \frac{|\mathbf{y}_i \cap \mathbf{y}_j|}{|\mathbf{y}_i \cup \mathbf{y}_j|}.$$

This loss is similar to the loss \mathcal{L}_{JSCL} introduced in [10]. The main difference lies in the position of the weight obtained through Jaccard similarity which is placed outside the logarithm. If kept inside, the coefficient has no impact on training ($\log(ax)$ and $\log(x)$ have the same derivative). It is also akin to the contrastive loss proposed in [30]. However, instead of employing Jaccard similarity, the authors utilized the conventional dot product.

In [20], the authors introduce a loss function that exclusively utilizes the interaction between instance representations and label prototypes to predict various types of educational content within a video. This type of contrastive loss, which forms pairs based solely on prototypes, closely resembles the classical Cross-Entropy loss [36, 37]. Here, the prototypes play a role analogous to the weight matrix of the final layer in a standard cross-entropy setup. The effectiveness of this loss raises the question of whether the performance gain is due to the optimization properties of contrastive learning or to the interactions among the instances.

We denote this loss as \mathcal{L}_{Proto} (2):

$$\mathcal{L}_{Proto} = -\frac{1}{|B|} \sum_{i \in \mathcal{B}} \frac{1}{|\Delta(\mathbf{z}_i)|} \sum_{j \in \Delta(\mathbf{z}_i)} \log \frac{\exp(\mathbf{z}_i \cdot \mathbf{c}_j)}{\sum_{\mathbf{c}_k \in \mathcal{C}} \exp(\mathbf{z}_i \cdot \mathbf{c}_k)} \quad (2)$$

It is worth noting that in their original paper, the authors do not evaluate the learned representations using standard approaches. Following the *SupCon* [24] method, we slightly modified the loss by incorporating all pairwise interactions in the denominator. We were motivated to do this for two reasons: first, to align with the *SupCon* loss, and second, to include the term from the numerator in the denominator, which is essential for good convergence.

The MulSupCon loss [19] has demonstrated its efficiency in transfer learning for computer vision. Unlike previous works, it treats each instance as a separate sample for each label, outperforming more complex approaches such as the one proposed in [31].

$$\mathcal{L}_{MulSupCon} = -\frac{1}{\sum_{i \in \mathcal{B}} |\Delta(\mathbf{z}_i)|} \sum_{i \in \mathcal{B}} \ell_{MulSupCon}(\mathbf{z}_i) \quad (3)$$

where $\ell_{MulSupCon}(\mathbf{z}_i)$ is the individual loss for example i defined as:

$$\ell_{MulSupCon}(\mathbf{z}_i) = \sum_{j \in \Delta(\mathbf{z}_i)} \frac{1}{|P(j, i)|} \sum_{\mathbf{z}_l \in P(j, i)} \log \frac{\exp(\mathbf{z}_i \cdot \mathbf{z}_l)}{\sum_{\mathbf{z}_k \in \mathcal{B} \setminus \mathbf{z}_i} \exp(\mathbf{z}_i \cdot \mathbf{z}_k)}$$

The Multi-label Supervised Contrastive (MSC) loss [18] has shown strong performance in natural language processing tasks with long-tailed distributions. It identifies and addresses the *attraction-repulsion imbalance* issue by incorporating a re-weighting method based on label

frequency and mitigates the *lack of positives* by integrating a MoCo [23] queue and label prototypes.

$$\mathcal{L}_{MSC} = -\frac{1}{|B|} \sum_{\mathbf{z}_i \in \mathcal{B}} \frac{1}{|\mathbf{y}_i|} \sum_{j \in \Delta(\mathbf{z}_i)} \frac{1}{N(i, j)} \sum_{\mathbf{z}_l \in P(j, i) \cup \mathcal{C}} f(\mathbf{z}_i, \mathbf{z}_j) \log \frac{\exp(\mathbf{z}_i \cdot \mathbf{z}_l / \tau)}{\sum_{\mathbf{z}_k \in \mathcal{B} \cup \mathcal{C} \setminus \mathbf{z}_i} g_i(\mathbf{z}_k, \beta) \exp(\mathbf{z}_i \cdot \mathbf{z}_k / \tau)}$$

The functions f (as defined in Eq. (4)) and g (Eq. (5)) are used to address the issue of *attraction-repulsion imbalance*.

$$f(\mathbf{z}_i, \mathbf{z}_j) = \begin{cases} 1 & \text{if } \mathbf{z}_j \in \mathcal{C}, \\ \frac{1}{|\mathbf{y}_i \cup \mathbf{y}_j|} & \text{otherwise.} \end{cases} \quad (4)$$

$$g_i(\mathbf{z}_k, \beta) = \begin{cases} 1 & \text{if } \mathbf{z}_k \in \mathcal{C}, \\ \beta & \text{otherwise.} \end{cases} \quad (5)$$

3.4 Gradient Study

To analyze the gradient of the classical multi-label contrastive loss function described above, we adopt the standard notation used in *SupCon* [24]. Here, $P(i)$ denotes the set of indices for positive instances relative to instance \mathbf{z}_i , $N(i)$ denotes the set of indices for negative instances, and $A(i)$ denotes the set of indices in the batch excluding i . It is important to note that the definition of positive or negative pairs depends on the specific method employed.

It is worth noting that all multi-label contrastive losses such as \mathcal{L}_{Base} , \mathcal{L}_{Proto} or \mathcal{L}_{MSC} , except the MulSupCon loss [19], can be expressed as follows:

$$\begin{aligned} \mathcal{L}_{contrastive} &= \frac{1}{|B|} \sum_{\mathbf{z}_i \in \mathcal{B}} \ell(\mathbf{z}_i) \\ \ell(\mathbf{z}_i) &= -\frac{1}{\sum_{p \in P(i)} \lambda_p^i} \sum_{j \in P(i)} \lambda_j^i \log \frac{\exp(\mathbf{z}_j \cdot \mathbf{z}_i)}{\sum_{k \in A(i)} \exp(\mathbf{z}_k \cdot \mathbf{z}_i)} \end{aligned} \quad (6)$$

This formulation generalizes the *SupCon* loss [24], where λ_j^i represents the expected similarity score between the anchor i and the positive pair j . In the specific case of *SupCon* loss, λ_j^i is set to 1.

The gradient of $\ell(\mathbf{z}_i)$ with respect to the anchor \mathbf{z}_i is computed using Eq. 7, while $\frac{\partial \ell(\mathbf{z}_i)}{\partial \mathbf{z}_k}$ for a positive pair is given in Eq. 8, and for a negative pair in Eq. 9.

$$\frac{\partial \ell(\mathbf{z}_i)}{\partial \mathbf{z}_i} = \sum_{j \in P(i)} \left(-\frac{\lambda_j^i}{\sum_{p \in P(i)} \lambda_p^i} + \sigma_{j,i} \right) \mathbf{z}_j + \sum_{n \in N(i)} \sigma_{n,i} \mathbf{z}_n \quad (7)$$

$$\frac{\partial \ell(\mathbf{z}_i)}{\partial \mathbf{z}_k} = \left(-\frac{\lambda_k^i}{\sum_{p \in P(i)} \lambda_p^i} + \sigma_{k,i} \right) \mathbf{z}_k \quad \text{if } k \in P(i) \quad (8)$$

$$\frac{\partial \ell(\mathbf{z}_i)}{\partial \mathbf{z}_k} = \sigma_{k,i} \mathbf{z}_k \quad \text{if } k \in N(i) \quad (9)$$

Where $\sigma_{j,i} = \frac{\exp(\mathbf{z}_j \cdot \mathbf{z}_i)}{\sum_{k \in A(i)} \exp(\mathbf{z}_k \cdot \mathbf{z}_i)}$.

The contrastive learning reaches its minimum when all previous gradients are zero, occurring when:

$$\sigma_{k,i} = \begin{cases} \frac{\lambda_k^i}{\sum_{p \in P(i)} \lambda_p^i} & \text{if } k \in P(i) \\ 0 & \text{if } k \in N(i) \end{cases} \quad (10)$$

This expression highlights the importance of properly defining the score between positive pairs and the definition of negative pairs.

3.5 Insights of previous works

In summary, recent approaches focus on key components such as the inclusion of prototypes [20, 18] and advancements in weighting positive pairs, as highlighted by the gradient study in the previous section. A common strategy for determining the weights of positive pairs involves considering label frequency, either by treating instances as individual labels [19] or by re-normalizing weights based on label frequency within the batch [18].

4 The Proposed Method

In this section, we introduce a new multi-label contrastive loss function, inspired by insights from previous work and our gradient analysis.

4.1 Observation

The effectiveness of contrastive learning for multi-label classification is highly sensitive to the choice of weighting coefficients, denoted as λ_j^i . Proper selection of these weights is crucial for achieving optimal results.

Interestingly, based on the gradients in Eq. (7), (8), and (9), we observe that under certain conditions, the gradient of a positive pair can mirror that of a negative pair, potentially hindering optimization.

Indeed, the gradient from a negative pair moves in the same direction as its representation \mathbf{z}_k , as observed in Eq. (9). Examining the form of a positive pair in Eq. (8) reveals that if the score $\sigma_{k,i}$ is sufficiently high, the term $\left(-\frac{\lambda_k^i}{\sum_{p \in P_i} \lambda_p^i} + \sigma_{k,i}\right)$ may become positive.

In this case, the gradient from a positive pair also moves in the same direction as its representation \mathbf{z}_k , causing the gradient to behave similarly to that of a negative example. A similar observation can be made by examining the gradient from positive and negative pairs in the derivation of the anchor in Eq. (7).

4.2 Regularized Loss

To counter this undesired behavior, we introduce a regularization term $\ell_{reg}(\mathbf{z}_i)$, which adjusts the gradient whenever a positive pair's gradient begins to resemble that of a negative pair (i.e., when $(-\Lambda_j^i + \sigma_{k,i}) > 0$).

For clarity, we define the normalized coefficient $\Lambda_j^i \in \mathbb{R}$ as:

$$\Lambda_j^i := \frac{\lambda_j^i}{\sum_{p \in P(i)} \lambda_p^i}$$

The regularization term $\ell_{reg}(\mathbf{z}_i)$ is defined as follows:

$$\ell_{reg}(\mathbf{z}_i) = - \sum_{j \in P(i)} \max(0, (-\Lambda_j^i + \sigma_{j,i} \cdot \text{detach}())) \mathbf{z}_j \cdot \mathbf{z}_i \quad (11)$$

where the `detach()` function excludes the gradient from this portion of the calculation.

This regularization term rebalances the gradient, ensuring that positive pairs remain distinct from negative pairs in terms of gradient behavior.

The gradients of $\ell_{reg}(\mathbf{z}_i)$ in relation to the anchor \mathbf{z}_i and the positive pair \mathbf{z}_k are computed in Eq. (12) and (13).

$$\frac{\partial \ell_{reg}(\mathbf{z}_i)}{\partial \mathbf{z}_i} = - \sum_{j \in P(i)} \mathbb{1}_{(-\Lambda_j^i + \sigma_{j,i}) > 0} (-\Lambda_j^i + \sigma_{j,i}) \mathbf{z}_j \quad (12)$$

$$\frac{\partial \ell_{reg}(\mathbf{z}_i)}{\partial \mathbf{z}_k} = -\mathbb{1}_{(-\Lambda_k^i + \sigma_{k,i}) > 0} (-\Lambda_k^i + \sigma_{k,i}) \mathbf{z}_k \quad (13)$$

This rebalances the gradient by replacing $\ell(\mathbf{z}_i)$ with $\hat{\ell}(\mathbf{z}_i)$ in Eq. (6).

$$\hat{\ell}(\mathbf{z}_i) = \ell(\mathbf{z}_i) + \ell_{reg}(\mathbf{z}_i) \quad (14)$$

The regularization loss $\ell_{reg}(\mathbf{z}_i)$ as shown in Fig 1, help in adjusting \mathbf{z}_k relative to \mathbf{z}_i by preventing excessively close positive pairs from causing unintended gradient effects. Notably, $\hat{\ell}(\mathbf{z}_i)$ and $\ell(\mathbf{z}_i)$ share the same minimum, as established in Eq. (10). Therefore, any improvement in performance arises purely from differences in optimization behavior.

4.3 Proposed Multi-Label Contrastive Loss Function

Our goal is to design a straightforward contrastive loss that incorporates our regularization term ℓ_{reg} , ensuring gradient adjustment based on previous insights. Following previous work [19, 18], we normalize the input based on label frequency within the batch and incorporate label prototypes, treating all prototypes in C as part of the batch \mathcal{B} . This approach, inspired by semi-supervised contrastive learning [36], enables prototypes to act as stable reference points for each label class.

We define our new multi-label regularized contrastive loss function, denoted \mathcal{L}_{REG} , defined as :

$$\mathcal{L}_{REG} = \frac{1}{|\mathcal{B}|} \sum_{\mathbf{z}_i \in \mathcal{B}} \hat{\ell}(\mathbf{z}_i) \quad (15)$$

Where,

$$\hat{\ell}(\mathbf{z}_i) := \frac{1}{|\mathbf{y}_i|} \sum_{j \in \Delta(\mathbf{z}_i)} \frac{1}{|P(j, i)|} \sum_{\mathbf{z}_l \in P(j, i)} \log \frac{\exp(\mathbf{z}_i \cdot \mathbf{z}_l)}{\sum_{\mathbf{z}_k \in \mathcal{B} \setminus \mathbf{z}_i} \exp(\mathbf{z}_i \cdot \mathbf{z}_k)} + \ell_{reg}(\mathbf{z}_i), \quad (16)$$

4.4 Taking Label Difference Between the Anchor and Positive Pair

As mentioned in [19], the attraction weights between instances are proportional to the number of shared labels between instances, weighted by the similarity of those labels. However, in some cases, the positive pair will contain labels that are not related to the anchor. Some works take this into account using the Jaccard Similarity [18, 10]. To account for varying levels of label overlap, we propose re-weighting the loss function based on the ratio of shared labels between the anchor and positive pairs :

$$f(\mathbf{y}_i, \mathbf{y}_j) = \left(\frac{|\mathbf{y}_i \cap \mathbf{y}_j|}{|\mathbf{y}_j|} \right)^\alpha, \quad (17)$$

where $\alpha \in \mathbb{R}^+$ controls the influence of label similarity. A higher α puts greater emphasis on these differences. This re-weighting refinement now gives the following loss definition:

$$\hat{\ell}(\mathbf{z}_i) = \frac{1}{|\mathbf{y}_i|} \sum_{j \in \Delta(\mathbf{z}_i)} \frac{1}{N(j, i)} \sum_{\mathbf{z}_l \in P(j, i)} f(\mathbf{y}_i, \mathbf{y}_l) \log \frac{\exp(\mathbf{z}_i \cdot \mathbf{z}_l)}{\sum_{\mathbf{z}_k \in \mathcal{B} \setminus \mathbf{z}_i} \exp(\mathbf{z}_i \cdot \mathbf{z}_k)} + \ell_{reg}(\mathbf{z}_i) \quad (18)$$

Where $N(j, i)$ is used to normalize the loss:

$$N(j, i) = \sum_{\mathbf{z}_l \in P(j, i)} f(\mathbf{y}_i, \mathbf{y}_l). \quad (19)$$

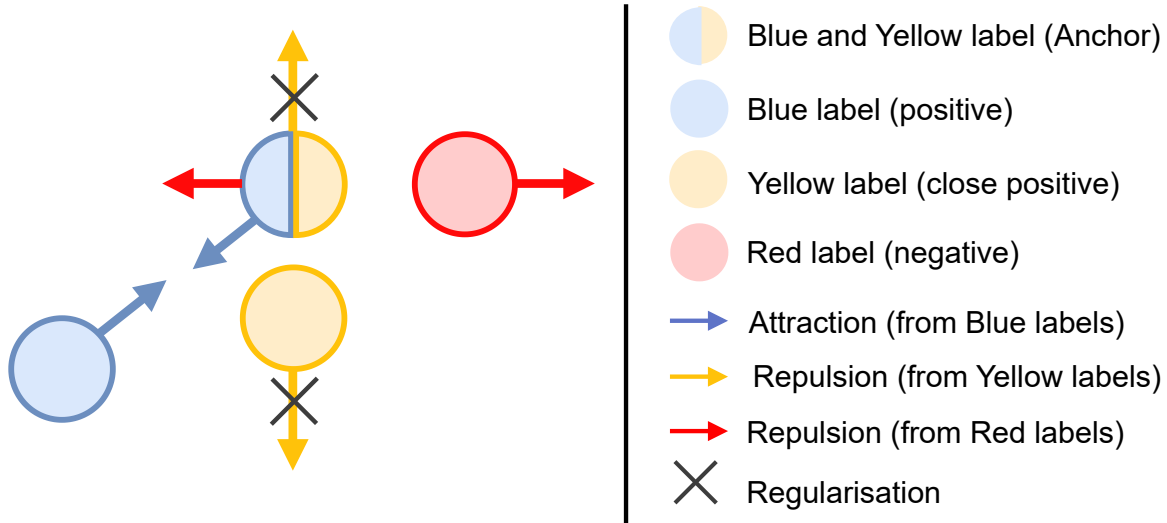


Figure 1: Visualization of gradient behavior in the multi-label contrastive loss: too close embeddings associated with Yellow label generate gradients causing unintended repulsion. Our proposed regularization adjusts these gradients, canceling the repulsion and ensuring proper attraction between similar examples.

5 Experimental Setup

This section starts with an introduction to the datasets used in our experiments. Following this, we will describe the baseline approaches against which we will compare our proposed balanced multi-label contrastive loss.

5.1 Datasets

For each dataset, we created a subset with limited training data to evaluate the performance of different approaches in a constrained setting.

5.1.1 Computer Vision

- **PASCAL VOC** [38]: This dataset includes images labeled with multiple object classes, with annotations covering 20 categories.
- **MS-COCO** [39]: The Microsoft Common Objects in Context (COCO) dataset contains images covering a wide range of everyday scenes and objects. Each image is annotated with 80 object categories.
- **NUS-WIDE** [40]: The NUS-WIDE dataset comprises Flickr images annotated with multiple tags from a set of 81 concepts.

5.1.2 Natural Language Processing

- **RCV1-v2** [41]: RCV1-v2 consists of categorized newswire stories provided by Reuters Ltd. Each newswire story can be assigned to multiple topics, with an initial total of 103 topics. We have retained the original training/test split, although we modified the number of labels.

- **AAPD** [7]: The Arxiv Academic Paper Dataset (AAPD) includes abstracts and associated subjects from 55,840 academic papers, where each paper may have multiple subjects.
- **BGC** [42]: The Blurb Genre Collection refers to a multi-label dataset comprising promotional descriptions of literary works.

For all image datasets which don’t have a fully released test set, we use the original train split to train the model, and divide the given validation set into 50/50 to create a true validation and test set. This approach helps to prevent data leakage and ensures that the test set remains entirely unseen during the model training and validation process (in particular for the small grid search performed during linear evaluation), leading to a more robust evaluation of model performance. Table 1 outlines the characteristics of these datasets.

Table 1: Datasets statistics for the standard split. The table shows the number of examples (in thousands) within the training, validation, and test sets, as well as the number of class labels L , the average number of labels per example \bar{L} . The letter ”S” refer to the subset version of the dataset used in low data regimes experiments.

	Dataset	Train	Val	Test	Train S	Val S	Test S	L	\bar{L}
Vision	PASCAL [38]	5.0k	2.5k	2.5k	1.0k	2.5k	2.5k	20	1.5
	COCO [39]	82.0k	20.2k	20.2k	16.4k	20.2k	20.2k	80	2.9
	NUS-WIDE [40]	125.4k	41.9k	41.9k	25.1k	41.9k	41.9k	81	2.4
NLP	RCV1 [41]	19.6k	3.4k	781.2k	4.9k	10.8k	788.6k	91	3.2
	AAPD [7]	37.8k	6.7k	11.3k	4.3k	16.3k	35.1k	54	2.4
	BGC [42]	58.7k	14.7k	18.3k	5.8k	30.6k	55.3k	146	3.0

5.2 Baseline

In this section, we first present the standard supervised loss functions used for multi-label classification.

5.2.1 Supervised Loss Function

- \mathcal{L}_{BCE} denotes the binary cross-entropy loss, computed as follows:

$$\mathcal{L}_{BCE} = -\frac{1}{N} \sum_{i=1}^N \frac{1}{L} \sum_{j=1}^L y_i^j \log(\hat{y}_i^j) + (1 - y_i^j) \log(1 - \hat{y}_i^j)$$

where, $\{\hat{y}_i^1, \dots, \hat{y}_i^L\}$ represent the model’s output probabilities for the instance i in the batch.

- \mathcal{L}_{ASY} represents the asymmetric loss function [16], computed as follows:

$$\mathcal{L}_{ASY} = -\frac{1}{N} \sum_{i=1}^N \frac{1}{L} \sum_{j=1}^L y_i^j (1 - s_i^j)^{\gamma^+} \log(s_i^j) + (1 - y_i^j) (s_i^j)^{\gamma^-} \log(1 - s_i^j) \quad (20)$$

with $s_i^j = \max(\hat{y}_i^j - m, 0)$. The parameter m corresponds to the hard-threshold, whereas γ^+ and γ^- are the down-weights.

- \mathcal{L}_{ZLPR} denotes the *Zero-bounded Log-sum-exp and Pairwise Rank-based* loss, computed as follows:

$$\mathcal{L}_{ZLPR} = \frac{1}{N} \sum_{i=1}^N \log(1 + \langle y_i, \exp(-s_i) \rangle) + \log(1 + \langle 1 - y_i, \exp(s_i) \rangle) \quad (21)$$

where s_i^j represents the logit of the j^{th} label for the i^{th} instance.

5.3 Implementation Details

The source code for this implementation is publicly available on GitHub¹. In all experiments, we implemented gradient clipping with a parameter value of 1. To reduce training and conserve memory, we employed 16-bit automatic mixed precision.

In the baseline, we employed a standard linear learning rate scheduler with a 5% warm up. During training, the model with the best Micro-F1 score is retained for testing, while the model that achieves the best average results (averaged over multiple seeds) on the validation set is also preserved for the testing phase. For the Asymmetric loss [16] we set $\gamma^+ = 0, \gamma^- = 1, m = 0$ following common practice [1].

For Contrastive Learning, as described in *SupCon* [24], we used a standard cosine learning rate scheduler with a 5% warm-up period and the temperature τ is set to 0.1. The projection head comprises two fully connected layers with ReLU as the activation function, defined as $W_2 \cdot \text{ReLU}(W_1 \cdot x)$, where $W_1 \in \mathbb{R}^{h \times h}$ and $W_2 \in \mathbb{R}^{d \times h}$. Here, h represents the dimension of the hidden space, and d is set to 256 in our experiments. To evaluate the model, we retain the last checkpoint of the model and discard the projection head. Subsequently, multiple logistic regression models are trained using binary cross-entropy (BCE) for each individual label.

The evaluation of results is conducted on the test set using traditional metrics, namely the Hamming loss, Micro-F1 score and Macro-F1 score [18].

5.3.1 Natural Language processing

For NLP experiments, no data augmentation was used, and documents were truncated to 220 tokens. Following previous works [17, 34], we employed encoder-only model, selecting RoBERTa-base [43] as the backbone, implemented via Hugging Face’s resources². In all experiments, the pre-trained model retained a dropout rate of 0.1, and bias and LayerNorm parameters were exempted from weight decay. The [CLS] token was used as the final text representation, with a fully connected layer serving as the decoder. We used the AdamW optimizer [44] with a weight decay of 0.01, excluding weight decay for bias and LayerNorm parameters as is common practice.

5.3.2 Computer Vision

For all computer vision experiments, we used a ResNet-50 architecture [45] pre-trained on ImageNet [46] weights unless otherwise specified. The model was optimized using stochastic gradient descent (SGD) with momentum, with a batch size of 64 and an input image resolution of 224.

For data augmentation, we applied RandAugment with standard parameters ($n = 2, m = 9$) for both contrastive training and linear evaluation. According to *SupCon*, this configuration achieves results comparable to their best-performing setting, which used AutoAugment. To ensure a fair comparison, we used the same augmentation strategy for models trained with Binary Cross-Entropy (BCE)-based loss.

¹Coming soon

²<https://huggingface.co/roberta-base>

Table 2: Comparative analysis of multi-label loss functions on vision datasets (PASCAL, MS-COCO, and NUS-WIDE) and NLP datasets (AAPD, RCV1, BGC). Metrics used are Micro-F1 (μ -F₁), Macro-F1 (M-F₁), and Hamming Loss (multiplied by 10^3). The best results are highlighted in bold, including those that are not significantly different from the top-performing scores.

Loss	PASCAL			MS-COCO			NUS-WIDE			AAPD			RCV1			BGC		
	μ -F ₁	M-F ₁	Ham	μ -F ₁	M-F ₁	Ham	μ -F ₁	M-F ₁	Ham	μ -F ₁	M-F ₁	Ham	μ -F ₁	M-F ₁	Ham	μ -F ₁	M-F ₁	Ham
Non-Contrastive Losses																		
\mathcal{L}_{BCE}	83.40	80.93	2.41	62.23	48.17	2.13	65.18	16.08	1.72	73.39	59.59	22.73	88.30	75.80	81.68	80.46	65.05	78.48
\mathcal{L}_{ASY} [16]	83.84	81.60	2.44	65.06	52.56	2.08	65.50	14.62	1.74	73.51	59.78	22.99	88.12	74.72	83.26	80.49	65.67	79.06
\mathcal{L}_{ZLPR} [17]	83.37	80.88	2.42	70.43	63.88	1.83	70.47	38.02	1.61	73.64	59.7	22.62	88.52	76.48	80.03	80.91	66.53	76.96
Contrastive Losses																		
\mathcal{L}_{Base} [10]	82.53	79.86	2.57	69.81	64.22	1.97	71.07	52.84	1.64	73.53	60.13	23.39	87.95	74.89	85.83	80.63	62.78	78.50
\mathcal{L}_{Proto} [20]	81.85	79.75	2.69	71.88	67.35	1.86	71.79	56.03	1.62	73.59	61.02	23.79	88.3	77.23	83.61	80.52	65.49	80.39
$\mathcal{L}_{MulSupCon}$ [19]	82.75	80.26	2.53	71.33	66.25	1.88	71.88	54.36	1.61	73.64	60.52	23.28	88.47	76.96	82.04	81.00	64.81	77.36
\mathcal{L}_{MSC} [18]	82.56	80.39	2.58	71.96	67.54	1.85	72.02	56.13	1.60	73.68	60.67	23.49	88.41	77.36	82.51	81.07	65.89	76.87
$\mathcal{L}_{W/O-REG}$	82.23	79.99	2.63	71.78	67.50	1.86	71.99	56.59	1.61	73.62	60.88	23.50	88.43	77.24	81.97	81.03	66.00	77.28
\mathcal{L}_{REG} (Eq. 15)	83.08	80.57	2.52	72.19	68.03	1.83	72.05	56.52	1.60	73.72	61.28	23.57	88.41	77.45	82.68	80.83	66.66	78.44

For non-contrastive losses, we trained for 5, 10, and 20 epochs, selecting the best-performing model based on validation performance. For contrastive learning methods, which demonstrated faster convergence and lower risk of overfitting, we consistently used 10 epochs. Given the impact of augmentation choice on contrastive learning, we leave the exploration of alternative augmentation strategies as a potential direction for future research.

In all the experiments, we chose to remove the MoCo [23] to effectively compare all contrastive loss without implementation trick. Additional implementation details can be found in the Appendix A.1.

6 Results

In this results section, we will describe the outcomes obtained on the full dataset, followed by an analysis of the results obtained on lower data regimes, with less training data.

6.1 Full Dataset

6.1.1 Standard Supervised Loss

For the standard supervised contrastive loss, we observed that when the number of labels is high, specifically higher than 80, the \mathcal{L}_{ZLPR} loss outperforms both the \mathcal{L}_{ASY} and \mathcal{L}_{BCE} loss functions across all metrics. This underscores the ability of this loss function to handle larger and more complex label interactions, in contrast to BCE-based losses. This can be explained by the fact that when the number of labels is high, the ratio between the number of positive and negative labels becomes lower, and BCE-based loss functions are known to struggle in such settings [16]. However, when the number of labels is lower, as is the case with PASCAL and AAPD, the performance of the asymmetric loss function is either equivalent to or better than that of the \mathcal{L}_{ZLPR} loss function. This result on a small number of labels is confirmed by further analysis experiments in Appendix A.5.

6.1.2 Contrastive Losses

In supervised contrastive learning setting on image dataset, our proposed loss function, \mathcal{L}_{REG} (Eq. 15), outperforms previous methods in almost all metrics. For natural language processing, the results are somewhat more mixed. The \mathcal{L}_{REG} loss achieves better results in terms of Macro-F1, but slightly lower results in terms of Micro-F1.

Table 3: Low data regime Comparative analysis of multi-label loss functions on vision datasets (PASCAL, MS-COCO, and NUS-WIDE) taking 20% of training examples and NLP datasets (AAPD, RCV1, BGC). Metrics used are Micro-F1 (μ -F₁), Macro-F1 (M-F₁), and Hamming Loss (multiplied by 10³). The best results are highlighted in bold, including those that are not significantly different from the top-performing scores.

Loss	PASCAL			MS-COCO			NUS-WIDE			AAPD			RCV1			BGC		
	μ -F ₁	M-F ₁	Ham	μ -F ₁	M-F ₁	Ham	μ -F ₁	M-F ₁	Ham	μ -F ₁	M-F ₁	Ham	μ -F ₁	M-F ₁	Ham	μ -F ₁	M-F ₁	Ham
Non-Contrastive Losses																		
\mathcal{L}_{BCE}	75.27	66.17	3.32	54.07	34.10	2.46	67.38	24.57	1.69	68.76	49.49	25.93	86.90	70.39	93.10	74.28	49.61	100.58
\mathcal{L}_{ASY}	77.03	71.04	3.28	57.22	39.59	2.43	68.69	27.43	1.68	68.85	51.40	27.22	86.91	72.34	90.54	74.64	52.29	103.35
$\mathcal{L}_{\text{ZLPR}}$	78.73	74.96	2.96	65.71	57.79	2.07	69.10	43.63	1.68	69.45	50.98	25.69	87.39	72.05	88.20	75.49	53.22	98.37
Contrastive Losses																		
$\mathcal{L}_{\text{Base}}$	79.21	76.19	3.07	64.83	58.35	2.36	68.54	47.68	1.82	69.42	49.85	26.13	86.62	71.03	95.28	75.26	51.75	9.865
$\mathcal{L}_{\text{Proto}}$	78.63	75.91	3.15	66.50	60.99	2.25	69.02	49.69	1.79	69.09	51.05	27.79	86.52	72.91	97.59	74.82	53.38	10.52
$\mathcal{L}_{\text{MulSupCon}}$	78.94	76.36	3.10	66.02	59.86	2.27	68.98	48.16	1.79	69.39	49.01	25.70	86.96	71.84	93.00	75.57	51.93	97.74
\mathcal{L}_{MSC}	78.83	76.59	3.17	66.34	60.65	2.26	69.19	49.64	1.78	69.45	50.69	26.77	86.91	72.49	94.16	75.63	52.57	97.69
$\mathcal{L}_{\text{W/O-REG}}$	78.59	76.16	3.20	66.46	61.06	2.25	69.37	50.19	1.75	69.23	49.95	26.41	86.77	72.17	94.46	75.51	52.82	98.91
\mathcal{L}_{REG}	79.63	76.77	3.02	67.04	61.90	2.20	69.63	50.39	1.75	68.89	52.30	29.11	86.5	73.09	97.77	75.21	53.44	10.35

6.1.3 Comparison between Standard and Contrastive Loss

In terms of performance, when the number of labels is low, contrastive losses are generally outperformed by the standard loss function. However, as the number of labels increases, even simple contrastive losses become competitive, as is the case for the MS-COCO, NUS-WIDE, and AAPD datasets. Moreover, in this setting, our proposed \mathcal{L}_{REG} loss function (Eq. 15) outperforms BCE-based methods and is equivalent to the $\mathcal{L}_{\text{ZLPR}}$ loss function.

6.2 Low Data Regimes

We investigate the effectiveness of previous loss functions within a limited-data framework. This exploration is motivated by the need to optimize model performance in scenarios where data availability is constrained. Interestingly, the results observed under limited-data conditions mirror those from full-dataset experiments, with amplified effects. This amplification is most notable in the Macro-F1 score, where our proposed loss function consistently achieves superior performance.

Table 3 illustrates the performance metrics when only 20% of the training data is used. It highlights the robustness of various loss functions, with contrastive losses demonstrating competitive performance. Notably, our loss function achieves the highest Macro-F1 scores across most datasets, underscoring its efficacy under data-scarce conditions.

Figure 2 provides further insight, examining Macro-F1 performance as a function of the fraction of training data retained. Two vision datasets, including PASCAL, are analyzed in this context. The key observations are as follows:

Contrastive losses maintain higher Macro-F1 scores as the training fraction decreases. This resilience is particularly evident in the PASCAL dataset, known for its smaller size and higher difficulty in low-data regimes. The smaller size of the PASCAL dataset exacerbates the impact of reduced training data. Nevertheless, contrastive loss functions preserve their discriminative power better than traditional approaches, enabling superior performance under sparse training conditions. Traditional non-contrastive losses struggle to maintain robust performance with limited training examples, underscoring the advantage of contrastive methods in leveraging sparse data effectively.

Key Takeaway The results indicate that contrastive loss functions are particularly well-suited for scenarios with limited data, achieving consistent performance across varying training

fractions. Their robustness and ability to exploit sparse training data make them a valuable tool for low-data machine learning challenges, especially in vision tasks.

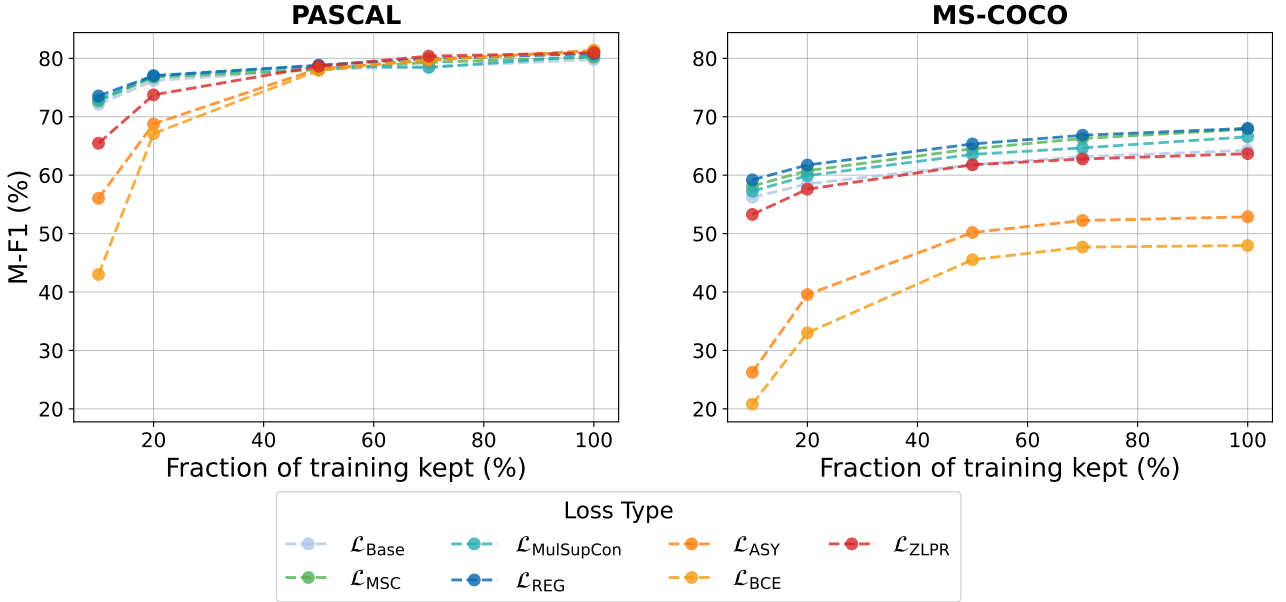


Figure 2: Macro-F1 under limited data conditions as a function of training set size: Contrastive losses demonstrate higher resilience to data scarcity.

6.3 Overall analysis

6.3.1 Confirmation of previous results

Previous works [18, 19] showed that taking account label frequency of positive pair and adding prototypes can improve the results. Our results validate this hypothesis. When comparing \mathcal{L}_{Base} and $\mathcal{L}_{MulSupCon}$, neither of these losses uses prototypes, and the crucial difference is that $\mathcal{L}_{MulSupCon}$ takes label frequency into account within the positive pair. Our results show that $\mathcal{L}_{MulSupCon}$ significantly outperforms \mathcal{L}_{Base} , especially in terms of Macro-F1, which validates the hypothesis. Our results also confirm that adding prototypes improves performance, especially in terms of Macro-F1. Other losses that use prototypes generally achieve better results in this metric compared to those that do not. Another indication of this is that our ablation study, \mathcal{L}_{MSCWRG} , based on insights from previous papers, performs very well across all datasets.

6.3.2 Prototypes

Among all the results obtained, one that stands out is from \mathcal{L}_{Proto} [20]. One of the major motivations behind supervised contrastive learning is that the loss intrinsically accounts for label interactions, which is not the case with previous standard supervised loss functions. However, \mathcal{L}_{Proto} does not respect this characteristic because it only involves label and prototype interactions. The results are surprising because this straightforward loss function, similar to the classical cross-entropy loss used in multi-class classification, achieves very high performance. This suggests that some of the results may be attributed not only to the fact that label interactions are considered, but also to the strong optimization process inherent in contrastive learning.

6.3.3 Ablation

To measure the effect of our proposed regularization, we compare the performance of \mathcal{L}_{REG} with its ablation, $\mathcal{L}_{\text{W/O-REG}}$. The results show that adding regularization leads to no loss or improvement in performance for Micro-F1, with an improvement in Macro-F1 specifically for natural language processing. Without loss of generality, our regularization approach can also be applied to the classical *SupCon* loss [24]. The results show that the regularization has no significant impact in the multi-class case (see Appendix A.4). We argue that our regularization term is effective only in the multi-label setting, as the definition of positive pairs is more complex in this case and requires regularization.

7 Analysis

In this section, we examine the optimization process of the contrastive learning loss function for multi-label classification.

We empirically study the representations learned by the contrastive loss function. To analyze the instance representations used for linear evaluation, we apply two metrics proposed in [47], which are shown to be asymptotically optimized by contrastive losses. The alignment loss, $\mathcal{L}_{\text{align}}$ (22), is defined as the expected distance between positive pairs. In the multi-label setting, we define positive pairs as instances that share exactly the same labels. The uniform loss, $\mathcal{L}_{\text{uniform}}$ (23), measures how uniformly the instance representations are distributed. Since both metrics are sensitive to vector norms, which can be adjusted through layer normalization, we normalize the feature representations.

$$\mathcal{L}_{\text{align}}(f) = \mathbb{E}_{(x,y) \sim p_{\text{pos}}} [\|f(x) - f(y)\|_2^2] \quad (22)$$

$$\mathcal{L}_{\text{uniform}}(f) = \log \mathbb{E}_{(x,y) \sim p_{\text{data}}} \left[e^{-2\|f(x) - f(y)\|_2^2} \right] \quad (23)$$

where f represents the feature mapping function, p_{pos} denotes the distribution of positive pairs, and p_{data} denotes the data distribution.

Table 4: Comparative Analysis of Representation Learned by Multi-Label Loss Functions on AAPD, PASCAL, and COCO Datasets. For both $\mathcal{L}_{\text{uniform}}$ and $\mathcal{L}_{\text{align}}$, **lower values are better**. **Best results are in bold**, second best are underlined.

Loss	PASCAL		COCO		AAPD	
	$\mathcal{L}_{\text{uniform}}$	$\mathcal{L}_{\text{align}}$	$\mathcal{L}_{\text{uniform}}$	$\mathcal{L}_{\text{align}}$	$\mathcal{L}_{\text{uniform}}$	$\mathcal{L}_{\text{align}}$
$\mathcal{L}_{\text{Base}}$	<u>-1.67</u>	<u>0.48</u>	-1.73	0.37	<u>-2.86</u>	0.72
$\mathcal{L}_{\text{Proto}}$	-1.61	0.54	-1.61	0.38	-2.07	0.25
$\mathcal{L}_{\text{MulSupCon}}$	<u>-1.69</u>	0.51	<u>-1.77</u>	<u>0.35</u>	-3.06	0.91
\mathcal{L}_{MSC}	-1.66	0.50	-1.71	0.37	-2.79	0.74
$\mathcal{L}_{\text{W/O-REG}}$	-1.60	0.54	-1.72	0.39	<u>-2.86</u>	0.81
\mathcal{L}_{REG} (Eq. 15)	-1.72	<u>0.40</u>	<u>-1.84</u>	<u>0.27</u>	-2.36	0.29

The results presented in Table 4 confirm our gradient analysis findings. For the COCO and Pascal datasets, our proposed loss \mathcal{L}_{REG} demonstrates better representation score across both $\mathcal{L}_{\text{uniform}}$ and $\mathcal{L}_{\text{align}}$ metrics. Specifically, \mathcal{L}_{REG} achieves the best scores on both metrics, outperforming other loss functions in terms of alignment while maintaining competitive uniformity.

On AAPD, compared to the ablation, \mathcal{L}_{REG} shows lower performance on the $\mathcal{L}_{\text{uniform}}$ metric but higher performance on $\mathcal{L}_{\text{align}}$. This can be explained by the fact that our regularization term mitigates repulsion dynamics. Additionally, $\mathcal{L}_{\text{Proto}}$ achieves the best score on $\mathcal{L}_{\text{align}}$ but the worst score on $\mathcal{L}_{\text{uniform}}$, emphasizing the importance of instance-instance interactions for achieving a strong $\mathcal{L}_{\text{uniform}}$ score.

8 Conclusion

In this paper, we conducted a comprehensive exploration of contrastive learning techniques for multi-label classification, providing valuable insights into their strengths and limitations. Our analysis of various contrastive loss functions across diverse training scenarios ranging from limited data to full dataset utilization demonstrates the adaptability of these methods and their effectiveness.

We highlighted that the success of contrastive learning in MLC arises not only from label interactions but also from its robust optimization properties. However, our investigation also uncovered critical limitations. Specifically, contrastive approaches exhibit suboptimal performance in datasets with fewer labels and on evaluation metrics focused on ranking, signaling the need for targeted advancements in these areas.

We proposed a novel contrastive loss function coupled with a gradient-based regularization technique. This approach not only leverages key findings from previous studies but also achieves state-of-the-art results in MLC benchmarks proposed for NLP and CV, demonstrating its practical efficacy and theoretical relevance.

While our work advances the understanding and performance of contrastive learning in multi-label classification, it also raises intriguing questions and opportunities for future exploration.

The strong performance obtained by using only prototypes opens an interesting avenue for research, with many possibilities. These include weighting the interactions differently between prototypes and instances or between instances themselves, as well as exploring alternative ways to optimize the prototypes.

The main distinction between the MulSupCon Loss and other approaches lies in the fact that instances with more labels are given greater weight within the loss. Investigating methods to weight instances differently, depending on the number of labels or positive pairs available within a batch, could also represent a promising direction for further research.

Another compelling avenue for exploration would be to develop alternative methods for evaluating the representation space. Current standard approaches rely on classical independent binary classification tasks, which do not account for ranking or label interactions during evaluation. Proposing evaluation strategies that better reflect these aspects could significantly enhance the assessment of learned representations.

9 References Section

References

- [1] Shilong Liu, Lei Zhang, Xiao Yang, Hang Su, and Jun Zhu. Query2label: A simple transformer way to multi-label classification. *arXiv preprint arXiv:2107.10834*, 2021.
- [2] Yova Kementchedjhieva and Ilias Chalkidis. An exploration of encoder-decoder approaches to multi-label classification for legal and biomedical text. In Anna Rogers, Jordan Boyd-Graber, and Naoaki Okazaki, editors, *Findings of the Association for Computational Linguistics: ACL 2023*, pages 5828–5843, Toronto, Canada, July 2023. Association for Computational Linguistics.
- [3] Ilias Chalkidis, Emmanouil Fergadiotis, Prodromos Malakasiotis, and Ion Androutsopoulos. Large-scale multi-label text classification on EU legislation. In Anna Korhonen, David Traum, and Lluís Màrquez, editors, *Proceedings of the 57th Annual Meeting of the Association for Computational Linguistics*, pages 6314–6322, Florence, Italy, July 2019. Association for Computational Linguistics.
- [4] Peng Xu, Zihan Liu, Genta Indra Winata, Zhaojiang Lin, and Pascale Fung. Emograph: Capturing emotion correlations using graph networks, 2020.
- [5] Huy-The Vu, Minh-Tien Nguyen, Van-Chien Nguyen, Minh-Hieu Pham, Van-Quyet Nguyen, and Van-Hau Nguyen. Label-representative graph convolutional network for multi-label text classification. *Applied Intelligence*, 2022.
- [6] Zhao-Min Chen, Xiu-Shen Wei, Peng Wang, and Yanwen Guo. Multi-label image recognition with graph convolutional networks. In *Proceedings of the IEEE/CVF conference on computer vision and pattern recognition*, pages 5177–5186, 2019.
- [7] Pengcheng Yang, Xu Sun, Wei Li, Shuming Ma, Wei Wu, and Houfeng Wang. SGM: sequence generation model for multi-label classification. In *Proceedings of the 27th International Conference on Computational Linguistics, COLING 2018, Santa Fe, New Mexico, USA, August 20-26, 2018*, 2018.
- [8] Vacit Oguz Yazici, Abel Gonzalez-Garcia, Arnau Ramisa, Bartlomiej Twardowski, and Joost van de Weijer. Orderless recurrent models for multi-label classification. In *Proceedings of the IEEE/CVF Conference on Computer Vision and Pattern Recognition*, pages 13440–13449, 2020.
- [9] Ximing Zhang, Qian-Wen Zhang, Zhao Yan, Ruifang Liu, and Yunbo Cao. Enhancing label correlation feedback in multi-label text classification via multi-task learning. *arXiv preprint arXiv:2106.03103*, 2021.
- [10] Nankai Lin, Guanqiu Qin, Gang Wang, Dong Zhou, and Aimin Yang. An effective deployment of contrastive learning in multi-label text classification. In *Findings of the Association for Computational Linguistics: ACL 2023*, Toronto, Canada, July 2023. Association for Computational Linguistics.
- [11] Jonatas Wehrmann, Ricardo Cerri, and Rodrigo Barros. Hierarchical multi-label classification networks. In *International conference on machine learning*, pages 5075–5084. PMLR, 2018.

- [12] Haibin Chen, Qianli Ma, Zhenxi Lin, and Jiangyue Yan. Hierarchy-aware label semantics matching network for hierarchical text classification. In *Proceedings of the 59th Annual Meeting of the Association for Computational Linguistics and the 11th International Joint Conference on Natural Language Processing (Volume 1: Long Papers)*, pages 4370–4379, 2021.
- [13] Lin Xiao, Xin Huang, Boli Chen, and Liping Jing. Label-specific document representation for multi-label text classification. In *Proceedings of the 2019 conference on empirical methods in natural language processing and the 9th international joint conference on natural language processing (EMNLP-IJCNLP)*, pages 466–475, 2019.
- [14] Tal Ridnik, Gilad Sharir, Avi Ben-Cohen, Emanuel Ben-Baruch, and Asaf Noy. Ml-decoder: Scalable and versatile classification head. In *Proceedings of the IEEE/CVF winter conference on applications of computer vision*, pages 32–41, 2023.
- [15] Tsung-Yi Lin, Priya Goyal, Ross Girshick, Kaiming He, and Piotr Dollár. Focal loss for dense object detection. In *Proceedings of the IEEE international conference on computer vision*, 2017.
- [16] Tal Ridnik, Emanuel Ben-Baruch, Nadav Zamir, Asaf Noy, Itamar Friedman, Matan Protter, and Lihi Zelnik-Manor. Asymmetric loss for multi-label classification. In *Proceedings of the IEEE/CVF International Conference on Computer Vision*, 2021.
- [17] Jianlin Su, Mingren Zhu, Ahmed Murtadha, Shengfeng Pan, Bo Wen, and Yunfeng Liu. Zlpr: A novel loss for multi-label classification. *arXiv preprint arXiv:2208.02955*, 2022.
- [18] Alexandre Audibert, Aurélien Gauffre, and Massih-Reza Amini. Exploring contrastive learning for long-tailed multi-label text classification. In *Proceedings of the European Conference on Machine Learning and Knowledge Discovery in Databases (ECMLPKDD)*, pages 245–261, 2024.
- [19] Pingyue Zhang and Mengyue Wu. Multi-label supervised contrastive learning. In *Proceedings of the AAAI Conference on Artificial Intelligence*, volume 38, pages 16786–16793, 2024.
- [20] Rohit Gupta, Anirban Roy, Claire Christensen, Sujeong Kim, Sarah Gerard, Madeline Cincebeaux, Ajay Divakaran, Todd Grindal, and Mubarak Shah. Class prototypes based contrastive learning for classifying multi-label and fine-grained educational videos. In *Proceedings of the IEEE/CVF conference on computer vision and pattern recognition*, pages 19923–19933, 2023.
- [21] Ting Chen, Simon Kornblith, Mohammad Norouzi, and Geoffrey Hinton. A simple framework for contrastive learning of visual representations. In *International conference on machine learning*, pages 1597–1607. PMLR, 2020.
- [22] Yuncheng Li, Yale Song, and Jiebo Luo. Improving pairwise ranking for multi-label image classification. In *Proceedings of the IEEE conference on computer vision and pattern recognition*, pages 3617–3625, 2017.
- [23] Kaiming He, Haoqi Fan, Yuxin Wu, Saining Xie, and Ross Girshick. Momentum contrast for unsupervised visual representation learning. In *Proceedings of the IEEE/CVF conference on computer vision and pattern recognition*, pages 9729–9738, 2020.
- [24] Prannay Khosla, Piotr Teterwak, Chen Wang, Aaron Sarna, Yonglong Tian, Phillip Isola, Aaron Maschinot, Ce Liu, and Dilip Krishnan. Supervised contrastive learning, 2021.

- [25] Florian Graf, Christoph Hofer, Marc Niethammer, and Roland Kwitt. Dissecting supervised contrastive learning. In *International Conference on Machine Learning*, pages 3821–3830. PMLR, 2021.
- [26] Varsha Suresh and Desmond Ong. Not all negatives are equal: Label-aware contrastive loss for fine-grained text classification. In Marie-Francine Moens, Xuanjing Huang, Lucia Specia, and Scott Wen-tau Yih, editors, *Proceedings of the 2021 Conference on Empirical Methods in Natural Language Processing*, pages 4381–4394, Online and Punta Cana, Dominican Republic, November 2021. Association for Computational Linguistics.
- [27] Zhenyu Zhang, Yuming Zhao, Meng Chen, and Xiaodong He. Label anchored contrastive learning for language understanding. In Marine Carpuat, Marie-Catherine de Marneffe, and Ivan Vladimir Meza Ruiz, editors, *Proceedings of the 2022 Conference of the North American Chapter of the Association for Computational Linguistics: Human Language Technologies*, pages 1437–1449, Seattle, United States, July 2022. Association for Computational Linguistics.
- [28] Jianggang Zhu, Zheng Wang, Jingjing Chen, Yi-Ping Phoebe Chen, and Yu-Gang Jiang. Balanced contrastive learning for long-tailed visual recognition. In *Proceedings of the IEEE/CVF Conference on Computer Vision and Pattern Recognition*, pages 6908–6917, 2022.
- [29] Jiequan Cui, Zhisheng Zhong, Shu Liu, Bei Yu, and Jiaya Jia. Parametric contrastive learning. In *Proceedings of the IEEE/CVF international conference on computer vision*, pages 715–724, 2021.
- [30] Xi’ao Su, Ran Wang, and Xinyu Dai. Contrastive learning-enhanced nearest neighbor mechanism for multi-label text classification. In *Proceedings of the 60th Annual Meeting of the Association for Computational Linguistics (Volume 2: Short Papers)*, Dublin, Ireland, May 2022. Association for Computational Linguistics.
- [31] Junwen Bai, Shufeng Kong, and Carla Gomes. Disentangled variational autoencoder based multi-label classification with covariance-aware multivariate probit model. In Christian Bessiere, editor, *Proceedings of the Twenty-Ninth International Joint Conference on Artificial Intelligence, IJCAI-20*, pages 4313–4321. International Joint Conferences on Artificial Intelligence Organization, 7 2020. Special track on AI for CompSust and Human well-being.
- [32] Shu Zhang, Ran Xu, Caiming Xiong, and Chetan Ramaiah. Use all the labels: A hierarchical multi-label contrastive learning framework. In *CVPR*, 2022.
- [33] Zihan Wang, Peiyi Wang, Lianzhe Huang, Xin Sun, and Houfeng Wang. Incorporating hierarchy into text encoder: a contrastive learning approach for hierarchical text classification. In *Proceedings of the 60th Annual Meeting of the Association for Computational Linguistics (Volume 1: Long Papers)*, Dublin, Ireland, May 2022.
- [34] Simon Chi Lok U, Jie He, Víctor Gutiérrez-Basulto, and Jeff Z. Pan. Instances and labels: Hierarchy-aware joint supervised contrastive learning for hierarchical multi-label text classification, 2023.
- [35] Son D. Dao, Ethan Zhao, Dinh Phung, and Jianfei Cai. Multi-label image classification with contrastive learning, 2021.

[36] Aurelien Gauffre, Julien Horvat, and Massih-Reza Amini. A unified contrastive loss for self-training. In *Machine Learning and Knowledge Discovery in Databases. Research Track and Demo Track*, pages 3–18, Cham, 2024. Springer Nature Switzerland.

[37] Kihyuk Sohn. Improved deep metric learning with multi-class n-pair loss objective. In D. Lee, M. Sugiyama, U. Luxburg, I. Guyon, and R. Garnett, editors, *Advances in Neural Information Processing Systems*, volume 29. Curran Associates, Inc., 2016.

[38] Mark Everingham, Luc Van Gool, Christopher KI Williams, John Winn, and Andrew Zisserman. The pascal visual object classes (voc) challenge. *International journal of computer vision*, 88:303–338, 2010.

[39] Tsung-Yi Lin, Michael Maire, Serge Belongie, James Hays, Pietro Perona, Deva Ramanan, Piotr Dollár, and C Lawrence Zitnick. Microsoft coco: Common objects in context. In *Computer Vision–ECCV 2014: 13th European Conference, Zurich, Switzerland, September 6–12, 2014, Proceedings, Part V 13*, pages 740–755. Springer, 2014.

[40] Tat-Seng Chua, Jinhui Tang, Richang Hong, Haojie Li, Zhiping Luo, and Yantao Zheng. Nus-wide: a real-world web image database from national university of singapore. In *Proceedings of the ACM international conference on image and video retrieval*, pages 1–9, 2009.

[41] David D Lewis. Rcv1-v2/lyrl2004: the lyrl2004 distribution of the rcv1-v2 text categorization test collection, 2004.

[42] Rami Aly, Steffen Remus, and Chris Biemann. Hierarchical multi-label classification of text with capsule networks. In Fernando Alva-Manchego, Eunsol Choi, and Daniel Khashabi, editors, *Proceedings of the 57th Annual Meeting of the Association for Computational Linguistics: Student Research Workshop*, pages 323–330, Florence, Italy, July 2019. Association for Computational Linguistics.

[43] Yinhan Liu, Myle Ott, Naman Goyal, Jingfei Du, Mandar Joshi, Danqi Chen, Omer Levy, Mike Lewis, Luke Zettlemoyer, and Veselin Stoyanov. Roberta: A robustly optimized bert pretraining approach. *arXiv preprint arXiv:1907.11692*, 2019.

[44] Ilya Loshchilov and Frank Hutter. Decoupled weight decay regularization. *arXiv preprint arXiv:1711.05101*, 2017.

[45] Kaiming He, Xiangyu Zhang, Shaoqing Ren, and Jian Sun. Deep residual learning for image recognition. In *Proceedings of the IEEE conference on computer vision and pattern recognition*, pages 770–778, 2016.

[46] Jia Deng, Wei Dong, Richard Socher, Li-Jia Li, Kai Li, and Li Fei-Fei. Imagenet: A large-scale hierarchical image database. In *2009 IEEE conference on computer vision and pattern recognition*, pages 248–255. Ieee, 2009.

[47] Tongzhou Wang and Phillip Isola. Understanding contrastive representation learning through alignment and uniformity on the hypersphere. In *International conference on machine learning*, pages 9929–9939. PMLR, 2020.

[48] Ken Lang. Newsweeder: Learning to filter netnews. In Armand Prieditis and Stuart Russell, editors, *Machine Learning Proceedings 1995*, pages 331–339. Morgan Kaufmann, San Francisco (CA), 1995.

[49] Saif Mohammad, Felipe Bravo-Marquez, Mohammad Salameh, and Svetlana Kiritchenko. Semeval-2018 task 1: Affect in tweets. In *Proceedings of the 12th international workshop on semantic evaluation*, pages 1–17, 2018.

A Appendix

A.1 Implementation Details

We train the standard loss functions, \mathcal{L}_{BCE} , \mathcal{L}_{ASY} , and \mathcal{L}_{ZLPR} , across multiple settings described in Table 5. For the contrastive loss, the evaluation of the representation space is based on the average outputs of three linear layers. For each label, we select the optimal learning rate and weight decay through a grid search, choosing based on validation performance. All hyperparameters for contrastive learning are detailed in Table 6.

Table 5: Hyperparameters used for standard supervised loss function

Dataset	Epochs	Learning Rate	Batch Size	Optimizer
PASCAL	{5,10,20}	0.003	64	SGD
MS-COCO	{5,10,20}	0.01	64	SGD
NUS-WIDE	{5,10,20}	0.01	64	SGD
AAPD & AAPD(S)	{10, 40, 80, 160}	{ $5e^{-5}$, $2e^{-5}$ }	{32, 64}	AdamW
RCV1 & RCV1 (S)	{10, 40, 80, 160}	{ $5e^{-5}$, $2e^{-5}$ }	{32, 64}	AdamW
BGC & BGC(S)	{10, 40, 80, 160}	{ $5e^{-5}$, $2e^{-5}$ }	{32, 64}	AdamW

Table 6: Hyperparameters used for supervised contrastive loss function

Dataset	Epochs	Learning Rate	Batch Size	α	Optimizer	Linear LR	Linear WD	Linear Batch Size	Linear Optimizer
PASCAL	10	0.003	64	0	AdamW	{1, $1e^{-1}$ }	{ $1e^{-1}$, $1e^{-2}$, $1e^{-4}$ }	64	AdamW
MS-COCO	10	0.01	64	0	SGD	{1, $1e^{-1}$ }	{ $1e^{-1}$, $1e^{-2}$, $1e^{-4}$ }	64	Adam
NUS-WIDE	10	0.01	64	0	AdamW	{1, $1e^{-1}$ }	{ $1e^{-1}$, $1e^{-2}$, $1e^{-4}$ }	64	RMSprop
AAPD	{320, 640}	{ $5e^{-5}$, $2e^{-5}$ }	256	{0, 1}	AdamW	{1, $1e^{-1}$ }	{ $1e^{-1}$, $1e^{-2}$, $1e^{-4}$, $1e^{-6}$ }	256	AdamW
RCV1	{320}	{ $5e^{-5}$, $2e^{-5}$ }	256	{0, 1}	AdamW	{1, $1e^{-1}$ }	{ $1e^{-1}$, $1e^{-2}$, $1e^{-4}$ }	256	AdamW
BGC	{320, 640}	{ $5e^{-5}$, $2e^{-5}$ }	256	{0, 1}	AdamW	{1, $1e^{-1}$ }	{ $1e^{-1}$, $1e^{-2}$, $1e^{-4}$, $1e^{-6}$ }	256	AdamW
AAPD (S)	{320, 640}	{ $5e^{-5}$, $2e^{-5}$ }	{128, 256}	{0, 1}	AdamW	{1}	{ $1e^{-2}$ }	256	AdamW
RCV1 (S)	{320, 640}	{ $5e^{-5}$, $2e^{-5}$ }	{128, 256}	{0, 1}	AdamW	{1}	{ $1e^{-2}$ }	256	AdamW
BGC (S)	{320, 640}	{ $5e^{-5}$, $2e^{-5}$ }	{128, 256}	{0, 1}	AdamW	{1}	{ $1e^{-2}$ }	256	AdamW

A.2 Impact of Temperature on the Positive Regularization Ratio

In this section, we study a key metric introduced on our introduced loss that we refer to as the *Positive Regularization Ratio (PRR)*. The PRR correspond the frequency with which our proposed regularization is applied to positive pairs, providing insights into how often the gradient correction mechanism is activated. Understanding the behavior of this ratio is essential, as it indicates whether the regularization term is effectively stabilizing positive pairs in a significant number of cases, or if it is only needed occasionally.

To investigate the impact of temperature on the PRR, we analyze different temperature values in the contrastive loss function. Note that in all our previous experiments on both vision and language datasets, the temperature parameter was set to 0.01. While this value has been effective in our preliminary evaluations, we leave a thorough exploration of its impact on overall performance and representation quality to future work. Temperature is a crucial hyperparameter in contrastive learning that scales the similarity scores, influencing how close or distant positive pairs are driven in the embedding space. We expect that lower temperatures, which tend to emphasize larger similarity differences, may result in higher PRR values, as instances with shared labels but low similarity scores may activate the regularization term more frequently. Conversely, higher temperatures may reduce the PRR by softening these differences.

Table 7 summarizes the results, showing the average PRR for various temperature values in our contrastive loss. This analysis provides a clearer understanding of how temperature tuning affects the regularization dynamics within our proposed loss function.

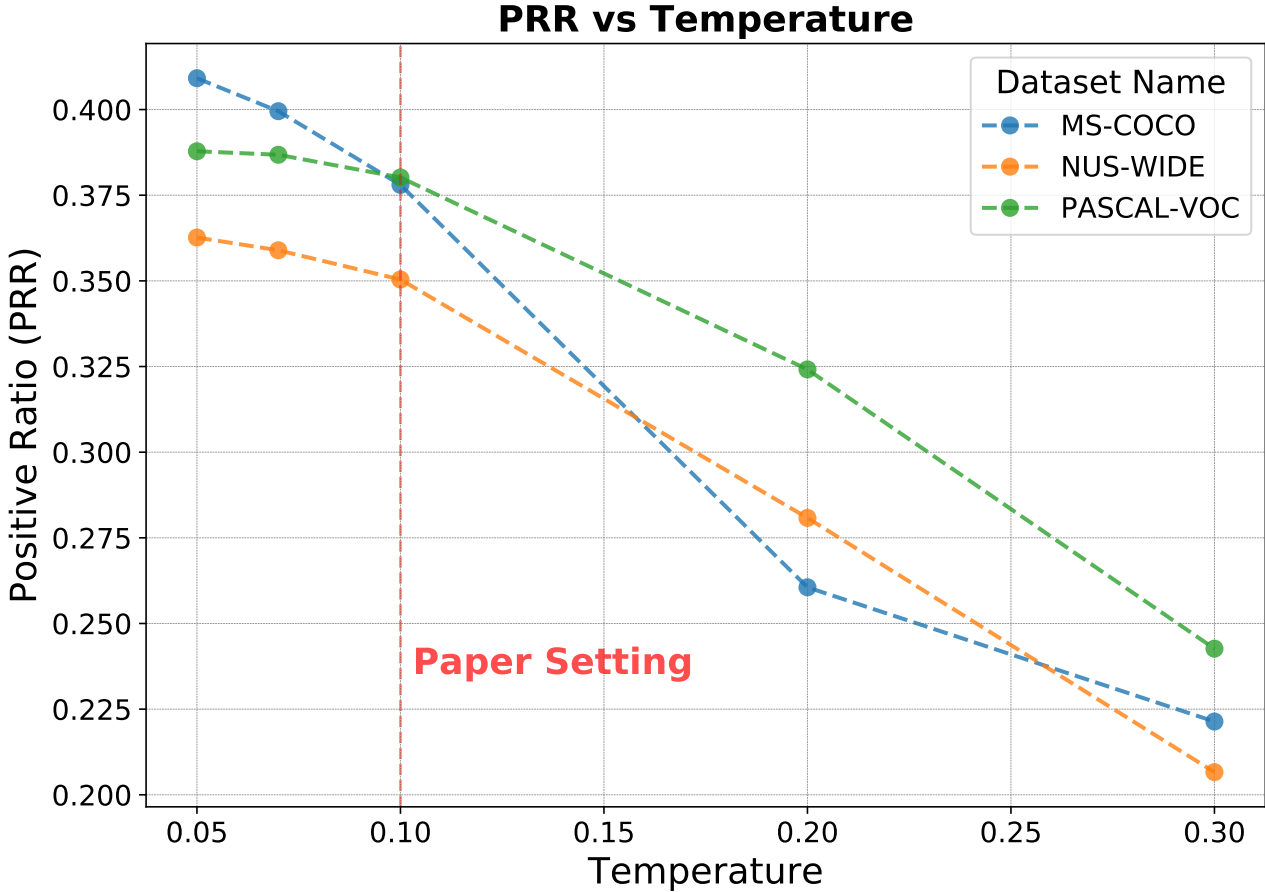


Table 7: Average Positive Regularization Ratio (PRR) as a function of temperature values in the contrastive loss. Lower temperatures increase PRR, suggesting a more frequent activation of the regularization term, while higher temperatures reduce PRR by minimizing differences in similarity scores.

Overall, we observe that the Positive Regularization Ratio (PRR) remains significant across different temperature values. In particular, at the temperature setting of 0.1, as used in this paper, the PRR is approximately 38%, indicating that our regularization term plays a crucial role in stabilizing the gradients for positive pairs.

A.3 Performance Across Training Epochs

We now analyze the behavior of different loss functions over varying numbers of training epochs, with particular attention to contrastive losses and their resilience to overfitting. In this setting, understanding how each loss function adapts to extended training is essential for identifying those that achieve stable performance over time. As illustrated in Figure 3, contrastive losses show a notable resistance to overfitting, consistently benefiting from longer training durations. This trend contrasts sharply with ZLPR or the baseline contrastive loss, which demonstrates signs of overfitting, particularly on the NUS-WIDE dataset. Interestingly, only a few epochs are required for contrastive losses to surpass ZLPR, underscoring their capacity for stable learning with extended epochs and highlighting their advantage in scenarios requiring prolonged training.

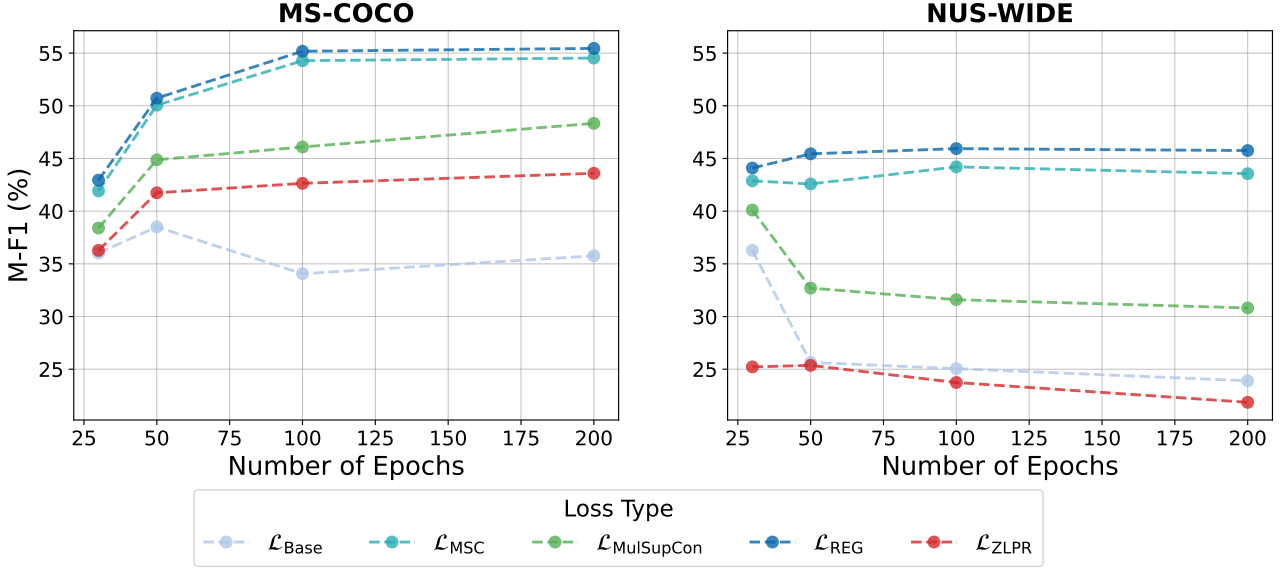


Figure 3: Performance across training epochs with random initialization: Contrastive losses display resilience to overfitting and benefit from extended training durations, whereas ZLPR shows signs of overfitting, particularly on the NUS-WIDE dataset.

A.4 Regularization applied on SupCon Loss

Our regularization method can also be applied to the classic *SupCon* [24] loss. The *SupCon* [24] loss can be written as follows:

$$\mathcal{L}_{\text{SupCon}} = \frac{1}{|B|} \sum_{\mathbf{z}_i \in \mathcal{B}} l_{\text{SupCon}}(\mathbf{z}_i) \quad (24)$$

$$l_{\text{SupCon}}(\mathbf{z}_i) = \frac{-1}{|P(i)|} \sum_{p \in P(i)} \log \frac{\exp(\mathbf{z}_i \cdot \mathbf{z}_p)}{\sum_{a \in A(i)} \exp(\mathbf{z}_i \cdot \mathbf{z}_a)}$$

Using the same principle as before, we can apply our regularization loss ℓ_{reg} to study the Supervised Contrastive Learning loss with gradient regularization, denoted as $\mathcal{L}_{\text{SupConReg}}$ (25).

$$\mathcal{L}_{\text{SupConReg}} = \frac{1}{|B|} \sum_{\mathbf{z}_i \in \mathcal{B}} \hat{l}_{\text{SupCon}}(\mathbf{z}_i) \quad (25)$$

$$\hat{l}_{\text{SupCon}}(\mathbf{z}_i) = \frac{-1}{|P(i)|} \sum_{p \in P(i)} \log \frac{\exp(\mathbf{z}_i \cdot \mathbf{z}_p)}{\sum_{a \in A(i)} \exp(\mathbf{z}_i \cdot \mathbf{z}_a)} + \ell_{reg}(\mathbf{z}_i)$$

We compare these loss functions on a single dataset, the 20 Newsgroups dataset [48], which contains approximately 18,000 newsgroup posts across 20 topics.

The results presented in Table 8 indicate that the performance of the cross-entropy loss and the *SupCon* loss is identical. Furthermore, incorporating our regularization does not lead to any noticeable improvement, yielding similar results.

Table 8: Comparison on Multi-Class Classification Loss function on NewsGroup dataset.

Loss	\mathcal{L}_{CE}	$\mathcal{L}_{\text{SupCon}}$	$\mathcal{L}_{\text{SupConRG}}$
NewsGroup			
Accuracy	86.60	86.68	86.64

Table 9: Datasets statistics for the standard split. The table shows the number of examples (in thousands) within the training, validation, and test sets, as well as the number of class labels L , the average number of labels per example \bar{L}

Dataset	Train	Val	Test	L	\bar{L}
SEMEVAL	6.6k	1.k	3.2k	11	2.4

A.5 Results on NLP dataset with a small number of labels

Regarding the PASCAL VOC 2007 dataset [39] in computer vision, which has a limited number of labels, we also applied our approach to the SemEval2018 dataset [49] in NLP. This dataset is used for multi-label emotion classification and includes only 11 labels, as shown in Table 9. The results Table 10 are consistent with those observed in the computer vision section. Notably, contrastive losses yield significantly lower performance, particularly in terms of Micro-F1, with the exception of our proposed loss, which achieves results comparable to conventional losses. On this dataset, the asymmetric loss outperforms other losses.

Table 10: Comparative analysis of multi-label loss functions on SemEval. Metrics used are Micro-F1 (μ -F₁), Macro-F1 (M-F₁), and Hamming Loss (multiplied by 10^3). The best results are highlighted in bold, including those that are not significantly different from the top-performing scores.

Loss	SemEval		
	μ -F ₁	M-F ₁	Ham
Non-Contrastive Losses			
\mathcal{L}_{BCE}	71.94	55.71	11.75
\mathcal{L}_{ASY}	72.43	57.68	11.95
\mathcal{L}_{ZLPR}	71.52	55.7	11.76
Contrastive Losses			
\mathcal{L}_{Base}	70.91	57.60	12.68
\mathcal{L}_{Proto}	69.99	56.08	12.89
$\mathcal{L}_{MulSupCon}$	70.83	57.06	12.67
\mathcal{L}_{MSC}	69.98	56.19	12.98
$\mathcal{L}_{W/O-REG}$	70.50	56.90	12.69
\mathcal{L}_{REG}	71.45	57.71	12.60

A.6 Ranking Metrics (mAP)

In this section, we provide results using a common evaluation metric in multi-label image classification: mean Average Precision (mAP). mAP measures the model’s ability to rank relevant labels higher than irrelevant ones for each instance.

Unlike contrastive loss, ZLPR focuses on learning representations for similarity or clustering, ZLPR optimizes the relative ordering of labels by penalizing cases where irrelevant labels are scored higher than relevant ones. This makes ZLPR fundamentally aligned with the objectives of ranking metrics like mAP as reflected in its superior mAP performance.

Table 11: mAP (Mean Average Precision) Comparative results of multi-label loss functions on VOC, COCO, and NUS-WIDE datasets using a pretrained Resnet-50. The best results are highlighted in bold, including those that are not significantly different from the top-performing scores.

	VOC	COCO	NUS-WIDE
Non-Contrastive Losses			
\mathcal{L}_{BCE}	87.44	64.18	38.00
\mathcal{L}_{ASY}	87.54	64.77	35.37
\mathcal{L}_{ZLPR}	87.19	71.74	54.85
Contrastive Losses			
\mathcal{L}_{Base}	80.09	65.92	51.25
\mathcal{L}_{Proto}	78.06	68.32	52.95
$\mathcal{L}_{MulSupCon}$	79.58	67.69	52.47
\mathcal{L}_{MSC}	80.02	68.38	52.87
$\mathcal{L}_{W/O-REG}$	78.27	68.12	52.79
\mathcal{L}_{REG}	79.24	68.96	53.61

A.7 Alpha Study

To address varying levels of label overlap, we propose re-weighting the loss function based on the ratio of shared labels between anchor and positive pairs, with the influence of this ratio controlled by a parameter α . While this adjustment aims to account for label correlations, the results show variability and appear to depend on the dataset. Consequently, α should be treated as a tunable hyperparameter, similar to others in the model.

A.8 Pseudo Code

Algorithm 1: Log Softmax with Temperature and denominator mask

Input: matrix: input matrix;
 τ : temperature;
mask ;
/* Apply temperature */
logits \leftarrow matrix/ τ ;
/* Apply exponential */
exp_logits \leftarrow exp(logits);
/* Row-wise softmax */
log_p \leftarrow logits - log((exp_logits \cdot mask).sum(dim=1));
/* Compute sigma */
 σ \leftarrow exp_logits/(exp_logits \cdot mask).sum(dim=1);
/* Return log softmax and sigma */
Output: log_p, σ .detach()

Algorithm 2: Multi-label Supervised Contrastive Learning with Gradient Regularization

Input: \mathbf{Z} : output features;
 \mathbf{Y} : labels;
 τ : temperature;
 E : small constant;

```
/* Create diagonal mask */  
mask_d ← ones( $\mathbf{Y}$ .shape[0] ×  $\mathbf{Y}$ .shape[0]);  
mask_d[0 :: (total + 1)] ← 0;  
mask_d ← mask_d.reshape( $\mathbf{Y}$ .shape[0],  $\mathbf{Y}$ .shape[0])  
/* Compute similarity */  
sim ←  $\mathbf{Z} \cdot \mathbf{Z}^T$ ;  
/* Compute weights */  
mask_and ← einsum('ac, bc → abc',  $\mathbf{Y}$ ,  $\mathbf{Y}$ );  
mask_and_d ← (mask_d.unsqueeze(2) · mask_and); norm ← mask_and_d.sum(dim=1);  
 $\lambda$  ← mask_and_d / (norm.unsqueeze(1) + E).sum(dim = 1);  
 $\Lambda$  ←  $\lambda / \mathbf{Y}$ .sum(dim = 1);  
/* Compute log softmax and sigma */  
logp,  $\sigma$  ← log_softmax_temp(sim,  $\tau$ , mask_d);  
/* Regularization term */  
mask_remove_g ← ( $\Lambda \neq 0$ ).float();  
weight_reg ← max( $-\Lambda + \sigma$ , 0) · mask_remove_g;  
reg ← weight_reg · sim/ $\tau$ ;  
/* Return final loss */  
Output:  $-(\log_p \cdot \lambda + \text{reg}) \cdot \text{sum}(\text{dim}=1) / \mathbf{Y}$ .shape[0]
```
